Targeted Online Liquid Chromatography Electron Capture Dissociation Mass Spectrometry for the Localization of Sites of in Vivo Phosphorylation in Human Sprouty2

Steve M. M. Sweet,[†] Faraz K. Mardakheh,[†] Kevin J. P. Ryan,[†] Amy J. Langton,[†] John K. Heath,[†] and Helen J. Cooper*

School of Biosciences, University of Birmingham, Edgbaston, Birmingham B15 2TT, U.K.

We demonstrate a strategy employing collision-induced dissociation for phosphopeptide discovery, followed by targeted electron capture dissociation (ECD) for site localization. The high mass accuracy and low background noise of the ECD mass spectra allow facile sequencing of coeluting isobaric phosphopeptides, with up to two isobaric phosphopeptides sequenced from a single mass spectrum. In contrast to the previously described neutral loss dependent ECD method, targeted ECD allows analysis of both phosphotyrosine peptides and lower abundance phosphopeptides. The approach was applied to phosphorylation analysis of human Sprouty2, a regulator of receptor tyrosine kinase signaling. Fifteen sites of phosphorylation were identified, 11 of which are novel.

Phosphorylation is a widespread and biologically significant protein post-translational modification.[1] Phosphopeptide discovery is becoming more routine, thanks largely to improved enrichment methods and higher speed mass spectrometers.[2,3] However site localization from collision-induced dissociation (CID) mass spectra remains a challenge, particularly for larger phosphopeptides with multiple potential phosphorylation sites.[4] Low-energy CID fragmentation of phosphopeptides frequently results in losses of phosphoric acid, in addition to the typical CID losses of water and ammonia, thus complicating manual analysis.[5–7] Bioinformatic approaches to automation of site localization have recently been published.[8,9] While automation streamlines the localization pro-

cess, many CID spectra still give ambiguous results, e.g., 39 and 33% of sites in two recent large-scale studies where confidence of site localization was quantified.[8,10] Site-directed mutagenesis is commonly used in order to decipher the functional significance of phosphorylation for a given protein.[11] If site-directed mutagenesis is to be carried out, obtaining accurate localization data for as many sites of phosphorylation as possible is particularly important, in order to avoid lengthy and costly analysis of inappropriate residues.

Alternative mass spectrometric methods for site localization include MS^3 of the H_3PO_4 neutral loss product ion, negative mode CID, and non-CID radical-driven fragmentation. Neutral loss dependent MS^3 spectra have been used to increase confidence in phosphopeptide identifications;[9,12–14] however, their contribution to site localization has not been rigorously described. Jiang et al. used information from paired MS^2 and MS^3 spectra to localize the site of phosphorylation, but neither the relative contributions to localization from the different scan types nor the confidence of site localization was reported.[12] Beausoleil et al. found that MS^3 spectra provided little additional localization information, an observation that was ascribed to reduced ion statistics in MS^3 spectra.[8] An additional caveat is that the neutral loss of water from unmodified residues results in a fragment of the same mass as loss of H_3PO_4 from a phosphorylated residue.[7,15] The use of negative ion mode CID to differentiate between clusters of potential phosphorylation sites has been described.[4] This method is based on a difference in intensity between two fragments, rather than distinct fragments.

Electron capture dissociation (ECD) and electron-transfer dissociation (ETD) are radical-driven fragmentation techniques.[16,17] In contrast to CID, labile modifications such as phosphorylation

---

* To whom correspondence should be addressed. Telephone: +44 (0)121 414 7527. Fax: +44 (0)121 414 5925. E-mail: H.J.Cooper@bham.ac.uk.
† CR-UK Growth Factor Group.

(1) Pawson, T.; Scott, J. D. *Trends Biochem. Sci.* **2005**, *30*, 286–290.
(2) Larsen, M. R.; Thingholm, T. E.; Jensen, O. N.; Roepstorff, P.; Jorgensen, T. J. D. *Mol. Cell. Proteomics* **2005**, *4*, 873–886.
(3) Collins, M. O.; Yu, L.; Choudhary, J. S. *Proteomics* **2007**, *7*, 2751–2768.
(4) Edelson-Averbukh, M.; Pipkorn, R.; Lehmann, W. D. *Anal. Chem.* **2007**, *79*, 3476–3486.
(5) Hunter, A. P.; Games, D. E. *Rapid Commun. Mass Spectrom.* **1994**, *8*, 559–570.
(6) Tabb, D. L.; Smith, L. L.; Breci, L. A.; Wysocki, V. H.; Lin, D.; Yates, J. R. *Anal. Chem.* **2003**, *75*, 1155–1163.
(7) Savitski, M. M.; Kjeldsen, F.; Nielsen, M. L.; Zubarev, R. A. *J. Proteome Res.* **2007**, *6*, 2669–2673.
(8) Beausoleil, S. A.; Villen, J.; Gerber, S. A.; Rush, J.; Gygi, S. P. *Nat. Biotechnol.* **2006**, *24*, 1285–1292.
(9) Olsen, J. V.; Blagoev, B.; Gnad, F.; Macek, B.; Kumar, C.; Mortensen, P.; Mann, M. *Cell* **2006**, *127*, 635–648.

(10) Li, X.; Gerber, S. A.; Rudner, A. D.; Beausoleil, S. A.; Haas, W.; Villen, J.; Elias, J. E.; Gygi, S. P. *J. Proteome Res.* **2007**, *6*, 1190–1197.
(11) Loyet, K. M.; Stults, J. T.; Arnott, D. *Mol. Cell. Proteomics* **2005**, *4*, 235–245.
(12) Jiang, X.; Han, G.; Feng, S.; Jiang, X.; Ye, M.; Yao, X.; Zou, H. *J. Proteome Res.* **2008**, *7*, 1640–1649.
(13) Yu, L.-R.; Zhu, Z.; Chan, K. C.; Issaq, H. J.; Dimitrov, D. S.; Veenstra, T. D. *J. Proteome Res.* **2007**, *6*, 4150–4162.
(14) Gruhler, A.; Olsen, J. V.; Mohammed, S.; Mortensen, P.; Faergeman, N. J.; Mann, M.; Jensen, O. N. *Mol. Cell. Proteomics* **2005**, *4*, 310–327.
(15) Lee, J.; Xu, Y.; Chen, Y.; Sprung, R.; Kim, S. C.; Xie, S.; Zhao, Y. *Mol. Cell. Proteomics* **2007**, *6*, 669–676.
(16) Zubarev, R. A.; Kelleher, N. L.; McLafferty, F. W. *J. Am. Chem. Soc.* **1998**, *120*, 3265–3266.

---

are retained on peptide backbone fragments upon ECD/ETD fragmentation.[18−21] This feature of ECD/ETD gives these methods a significant advantage over CID for the localization of phosphorylation sites.[21] ETD has recently been applied to the identification of large numbers of phosphopeptides in proteomic experiments.[22,23] ETD is performed predominantly on low-resolution ion trap mass spectrometers, and ambiguities arise from the possibility of fragment ions of the same nominal mass. Work is ongoing to implement ETD on an instrument with a high-resolution mass analyzer.[24,25] ECD has the advantage that mass spectra are acquired with high resolution and mass accuracy, as it is virtually exclusive to Fourier transform ion cyclotron resonance mass spectrometry. We have shown previously that online liquid chromatography (LC) ECD can be used in phosphopeptide discovery.[26] That method, neutral loss dependent ECD (NL ECD), takes advantage of the signature neutral loss of H_3PO_4 in order to focus ECD time on phosphopeptides. ECD has the potential to give excellent quality mass spectra of phosphopeptides, but it is unlikely to be as efficient as CID for phosphopeptide discovery, due to the requirement for accumulation of considerably greater amounts of precursor with concomitant increases in scan time.

In order to maximize the advantages of ECD, we now present an alternative application of ECD for site localization. Phosphopeptide discovery is carried out in an initial LC-CID experiment, followed by targeted LC-ECD of the identified phosphopeptides, enabling site localization and confirmation of the phosphopeptide identification. The use of an initial stage of mass spectrometry to generate an inclusion list for subsequent analysis has been applied previously to the identification of phosphopeptides and other substoichiometric components of a mixture.[27,28] Annan et al. employed negative ion mode precursor ion scanning, followed by positive ion mode MS/MS analysis of the resulting precursor ions.[28] Picotti et al. employed multiple rounds of targeted LC−CID MS/MS in order to identify low-abundance components of a protein digest.[27] In our targeted LC-ECD method, ECD analyses are not dependent on the presence of a CID neutral loss peak, allowing site localization of phosphotyrosine peptides (which do not show a dominant neutral loss). ECD events are restricted to a known number of phosphopeptides, allowing the ECD time to be extended to improve sequencing of low-abundance phosphopeptides: The least abundant phosphopeptide identified had a 200-fold lower intensity than the most abundant phosphopeptide. We apply this strategy to human Sprouty2, an important regulator of receptor tyrosine kinase signaling.[29] Sprouty2 has been shown to antagonize pathways downstream of fibroblast growth factor signaling.[29,30] Tyrosine phosphorylation (at Tyr55) has been shown to be essential for this antagonism; however, the mechanism by which this is accomplished is largely unknown.[29,31] Sprouty2 is downregulated in various cancers, suggesting it has a tumor-suppressor role.[32] In addition to tyrosine phosphorylation, Sprouty2 is known to be phosphorylated on serine and threonine residues.[30,33] Alterations in Sprouty2 phosphorylation, observed as a shift in SDS PAGE migration, have been implicated in Sprouty2 activity.[33−35] Precise localization of the sites of Sprouty2 phosphorylation will allow the role of phosphorylation in Sprouty2 function to be assessed further.

By use of targeted ECD, we were able to identify 14 sites of phosphorylation, 11 of which have not been described previously. Taking advantage of the high mass accuracy and low background noise levels of the ECD spectra, we demonstrate that up to two coeluting isobaric phosphopeptides can be assigned from a single ECD spectrum. ECD has been widely hailed as applicable to the analysis of phosphorylation.[20,21,36] While ECD has been applied to the identification of known sites of phosphorylation and to the identification of sites of phosphorylation on synthetic peptides,[21,36−38] this work is among the first applications of ECD to the assignment of novel sites of in vivo phosphorylation on a biologically significant signaling protein.[39,40]

EXPERIMENTAL METHODS

Plasmid Constructs. N-Terminally tagged Myc-human Sprouty2 (hSpry2) was constructed via Gateway cloning (Invitrogen Life Technologies). Briefly, the previously described hSpry2 (WT)−pEFBOS-ires-Topaz construct was used as template,[41] along with the following Gateway compatible forward and reverse primers:

(17) Syka, J. E.; Coon, J. J.; Schroeder, M. J.; Shabanowitz, J.; Hunt, D. F. *Proc. Natl. Acad. Sci. U. S. A* **2004**, *101*, 9528–9533.

(18) Cooper, H. J.; Håkansson, K.; Marshall, A. G. *Mass Spectrom. Rev.* **2005**, *24*, 201–222.

(19) Shi, S. D. H.; Hemling, M. E.; Carr, S. A.; Horn, D. M.; Lindh, I.; McLafferty, F. W. *Anal. Chem.* **2001**, *73*, 19–22.

(20) Stensballe, A.; Jensen, O. N.; Olsen, J. V.; Haselmann, K. F.; Zubarev, R. A. *Rapid Commun. Mass Spectrom.* **2000**, *14*, 1793–1800.

(21) Sweet, S. M. M.; Cooper, H. J. *Expert Rev. Proteomics* **2007**, *4*, 149–159.

(22) Molina, H.; Horn, D. M.; Tang, N.; Mathivanan, S.; Pandey, A. *Proc. Natl. Acad. Sci. U. S. A.* **2007**, *104*, 2199–2204.

(23) Chi, A.; Huttenhower, C.; Geer, L. Y.; Coon, J. J.; Syka, J. E. P.; Bai, D. L.; Shabanowitz, J.; Burke, D. J.; Troyanskaya, O. G.; Hunt, D. F. *Proc. Natl. Acad. Sci. U. S. A.* **2007**, *104*, 2193–2198.

(24) McAlister, G. C.; Phanstiel, D.; Good, D. M.; Berggren, W. T.; Coon, J. J. *Anal. Chem.* **2007**, *79*, 3525–3534.

(25) Williams, D. K.; McAlister, G. C.; Good, D. M.; Coon, J. J.; Muddiman, D. C. *Anal. Chem.* **2007**, *79*, 7916–7919.

(26) Sweet, S. M. M.; Creese, A. J.; Cooper, H. J. *Anal. Chem.* **2006**, *78*, 7563–7569.

(27) Picotti, P.; Aebersold, R.; Domon, B. *Mol. Cell. Proteomics* **2007**, *6*, 1589–1598.

(28) Annan, R. S.; Huddleston, M. J.; Verma, R.; Deshaies, R. J.; Carr, S. A. *Anal. Chem.* **2001**, *73*, 393–404.

(29) Hanafusa, H.; Torii, S.; Yasunaga, T.; Nishida, E. *Nat. Cell Biol.* **2002**, *4*, 850–858.

(30) Impagnatiello, M.-A.; Weitzer, S.; Gannon, G.; Compagni, A.; Cotten, M.; Christofori, G. *J. Cell Biol.* **2001**, *152*, 1087–1098.

(31) Li, X.; Wheldon, L.; Heath, J. K. *Biochem. Soc. Trans.* **2003**, *31*, 1445–1446.

(32) Lo, T. L.; Yusoff, P.; Fong, C. W.; Guo, K.; McCaw, B. J.; Phillips, W. A.; Yang, H.; Wong, E. S. M.; Leong, H. F.; Zeng, Q.; Putti, T. C.; Guy, G. R. *Cancer Res.* **2004**, *64*, 6127–6136.

(33) Lao, D.-H.; Yusoff, P.; Chandramouli, S.; Philp, R. J.; Fong, C. W.; Jackson, R. A.; Saw, T. Y.; Yu, C. Y.; Guy, G. R. *J. Biol. Chem.* **2007**, *282*, 9117–9126.

(34) Lao, D.-H.; Chandramouli, S.; Yusoff, P.; Fong, C. W.; Saw, T. Y.; Tai, L. P.; Yu, C. Y.; Leong, H. F.; Guy, G. R. *J. Biol. Chem.* **2006**, *281*, 29993–30000.

(35) DaSilva, J.; Xu, L.; Kim, H. J.; Miller, W. T.; Bar-Sagi, D. *Mol. Cell. Biol.* **2006**, *26*, 1898–1907.

(36) Kocher, T.; Savitski, M. M.; Nielsen, M. L.; Zubarev, R. A. *J. Proteome Res.* **2006**, *5*, 659–668.

(37) Woodling, K. A.; Eyler, J. R.; Tsybin, Y. O.; Nilsson, C. L.; Marshall, A. G.; Edison, A. S.; Al-Naggar, I. M.; Bubb, M. R. *J. Am. Soc. Mass Spectrom.* **2007**, *18*, 2137–2145.

(38) Abbott, K. L.; Renfrow, M. B.; Chalmers, M. J.; Nguyen, B. D.; Marshall, A. G.; Legault, P.; Omichinski, J. G. *Biochemistry* **2005**, *44*, 2732–2745.

(39) Kjeldsen, F.; Savitski, M. M.; Nielsen, M. L.; Shi, L.; Zubarev, R. A. *Analyst* **2007**, *132*, 768–776.

(40) Zabrouskov, V.; Ge, Y.; Schwartz, J.; Walker, J. W. *Mol. Cell. Proteomics* **2008**, M700524−MCP700200.

(41) Li, X.; Brunton, V. G.; Burgar, H. R.; Wheldon, L. M.; Heath, J. K. *J. Cell Sci.* **2004**, *117*, 6007–6017.

Table 1. Sprouty2 Phosphopeptides Identified from Initial LC−CID MS/MS[a]

phosphopeptide[b]	site	number of potential sites	precursor m/z (charge state)	precursor mass accuracy (ppm)	Mascot Expect value[c]	Site localized? (Ascore)[d]
R.AQpSGN*GSQPLLQTPR.D	Ser 7	3	817.88(2)	1.5	0.0012	yes (66.7)
R.DALTQQVHVLpSLDQIR.A	Ser 42	2	958.49(2)	0.9	6.6×10^{-4}	yes (127.5)
R.NTNEYpTEGPTVVPR.P	Thr 56	4	828.87(2)	7.6	34†	no (0)
R.SISTVSpSGSR.S	Ser 116	6	530.74(2)	7.0	0.14†	no (7.93)
R.LLGSSFpSSGPVADGIIR.V	Ser 141	4	878.44(2)	0.4	7.6×10^{-7}	no (16.2)
K.SELKPGELKPLpSK.E	Ser 167	2	753.40(2)	3.8	0.0062	yes (89.8)
K.VPpTVPPR.N	Thr 305	1	423.22(2)	0.9	0.018	yes (n/a)

[a] Mascot scores were above the threshold for identity or extensive homology, except where indicated as †. (Identification was confirmed by subsequent ECD fragmentation). [b] Lowercase p indicates phosphorylation throughout. * indicates deamidation. [c] Mascot Expect value indicates the number of times a random equal or higher score could be expected ($p > 0.05$). [d] Ascore algorithm was used to assess site localization: Ascore ≥20 indicates confident localization ($p = 0.01$).[8]
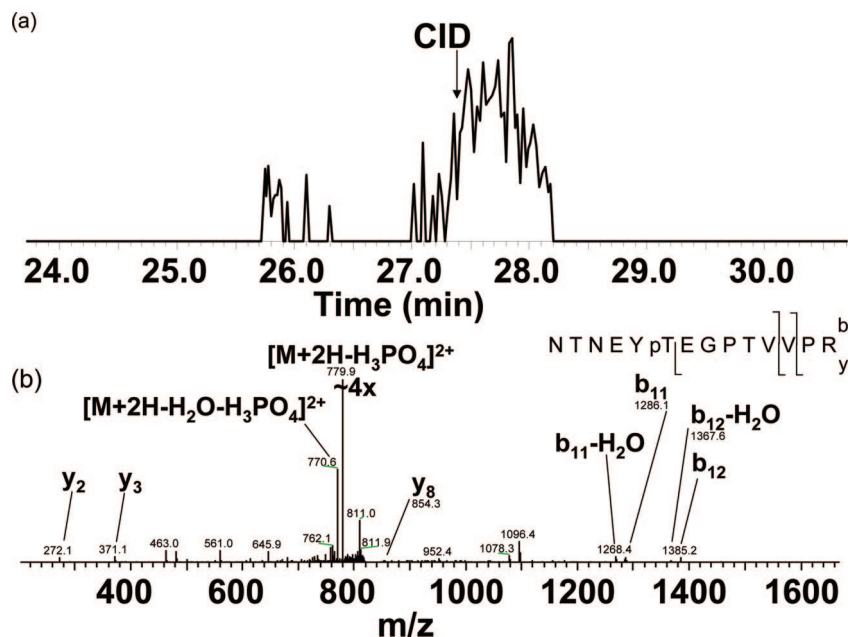

Figure 1. Online nanoLC separation of Sprouty2 tryptic digest, after phosphopeptide enrichment, with data-dependent CID of phosphorylated NTNEY[55]TEGPTVVPR. (a) Extracted ion chromatogram, showing elution of phosphorylated NTNEY[55]TEGPTVVPR, as $[M + 2H]^{2+}$ ions. The arrow marks the selection of these precursor ions for CID. (b) CID fragmentation of $[M + 2H]^{2+}$ ions of phosphorylated NTNEY[55]TEGPTVVPR. Lowercase p indicates phosphorylation. Inset: observed backbone fragments.

(G G G G A C A A G T T T G T A C A A A A A A G C A G G C T-TGATGGAGGCCAGAGCTCAGAGTG, and GGGGACCACTTTG-TACAAGAAAGCTGGGTCCTATGTTGGTTTTTCAAAGTTC) in a PCR to synthesize a hSpry2 coding fragment with in-frame gateway sequence overhangs. The product was subsequently recombined into GatewaypDONR201 entry vector (Invitrogen), using BP clonase enzyme (Invitrogen). Myc tagged hSpry2 was then generated by recombining hSpry2 from pDONR201 entry vector into a Myc-pRK5 gateway mammalian expression vector (kindly provided by Laura M. Machesky, University of Birmingham), using LR clonase enzyme (Invitrogen).

Reagents and Antibodies. Mouse monoclonal anti-c-Myc (clone 9E10) antibody was provided from Cancer Research UK (CRUK) Research Monoclonal Antibody Service. Horseradish peroxidase conjugated secondary anti- mouse IgG antibodies were purchased from Amersham Biosciences Inc. Protein-G coupled Sepharose beads were purchased from Sigma Aldrich (Gillingham, Dorset, UK). TiO₂ Titansphere beads (5-μm diameter) were obtained from GL Sciences (Japan).

Cell Culture, Transient Transfection, and Immunoprecipitation. Human embryonic kidney epithelial 293T cells were cultured at 37 °C, 5% CO₂ in Dulbeccos Modified Eagle Medium (Invitrogen) supplemented with 10% fetal bovine serum (v/v) (Labtech International). Transfections were performed using GeneJuice transfection reagent (Novagen) according to the manufacturer's instructions. Cells were incubated for 36 h after transfection to allow sufficient expression of the recombinant proteins. The efficiency of transfection was monitored using a GFP transfected positive control and was at all times >50%. Following transfections, cells were lysed with ~3 μL of ice-cold lysis buffer/cm² of confluent cells (50 mM Tris pH 7.5, 1 mM EDTA pH 7.5, 150 mM NaCl, 0.5% TritonX-100 (v/v), 1 mM Na₃VO₄, 50 mM NaF, 1 mM phenylmethanesulfonyl fluoride, and 1 tablet of complete mini protease inhibitor cocktail (Roche Diagnostics) for every 10 mL of buffer) Lysates were subsequently cleared by centrifugation at 14000g for 20 min. All steps were performed at 4 °C. Total protein concentrations of the cleared lysates were then determined by Coomassie (Bradford) Protein Assay Kit (Pierce Biotechnology
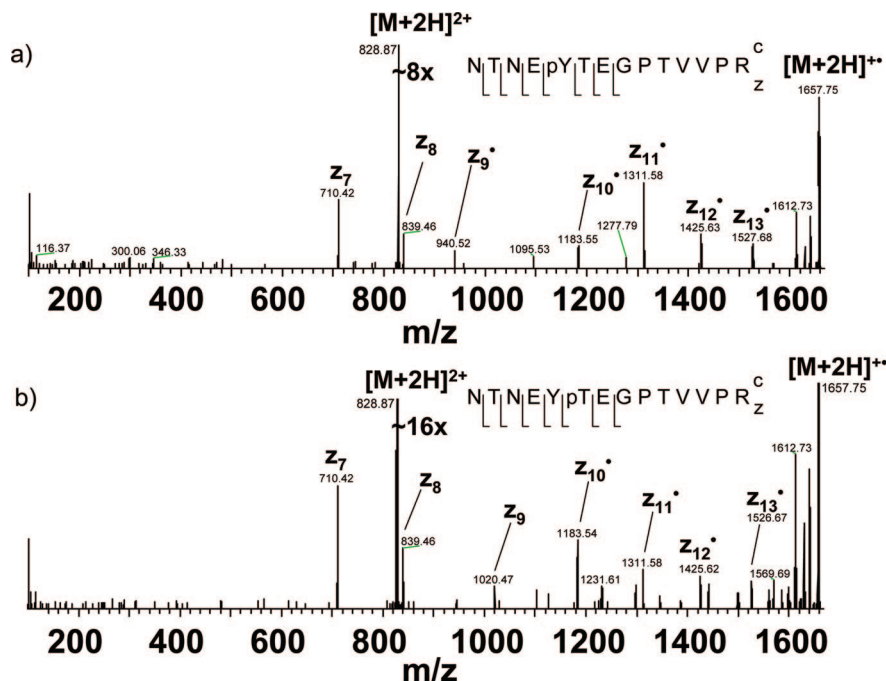
Figure 2. Online nanoLC targeted ECD of $[M + 2H]^{2+}$ ions of phosphorylated NTNEY[55]TEGPTVVPR. ECD mass spectra of $[M + 2H]^{2+}$ ions of phosphorylated NTNEY[55]TEGPTVVPR (a) at retention time 26.2 min and (b) at retention time 27.6 min. ECD mass spectra comprise 24 coadded microscans. Inset: observed backbone fragments.

Inc.), according to the manufacturer's instructions. For immunoprecipitation, ~50 μg of anti-Myc antibody was directly added to ~7 mg of lysate and incubated for 6 h at 4 °C with gentle agitation, followed by addition of 100 μL of 50% washed protein G-Sepharose fast flow slurry (Amersham Biosciences Inc.). The mixture was then further incubated for 16 h at 4 °C. After incubation, beads were washed 5 times with ice-cold lysis buffer (20× the bed volume of the beads), before being resuspended and boiled for 5 min in 2× SDS PAGE sample buffer (10% glycerol (v/v), 2% SDS (w/v), 0.1% bromophenol blue (w/v), 200 mM 1, 4-dithiothreitol (DTT), 100 mM Tris HCl, pH 6.8). Samples were then resolved on 4−12% precast NuPAGENovex Bis-Tris gels (Invitrogen) using NuPAGE-MOPS SDS Running Buffer (Invitrogen), and protein bands were visualized by staining with ImperialProtein Coomassie stain (Pierce Biotechnology Inc.) for 1 h.

In-Gel Digestion and Phosphopeptide Enrichment. Following Coomassie staining, the Sprouty2 band was excised. Cysteines were reduced (10 mM DTT) and alkylated (50 mM iodoacetamide) prior to overnight in-gel trypsin digestion (12.5 ng/μL; Trypsin Gold; Promega, Madison, WI) in 25 mM ammonium bicarbonate.

Phosphopeptides were enriched from the resulting mixture by TiO$_2$ affinity chromatography according to Larsen et al.,[2] with minor modifications. Peptides were loaded onto TiO$_2$ microcolumns in 2% trifluoroacetic acid (TFA). Columns were washed with 100 mg/mL 2,5-dihydroxybenzoic acid (DHB), 80% MeCN, 2% TFA, then with the same buffer omitting DHB. Peptides were eluted in a two-step procedure with 50 mM Na$_2$HPO$_4$ followed by dilute NH$_4$OH solution. Eluates were desalted using C18 ZipTips, according to the manufacturer's instructions (Millipore). The resulting peptide mixtures were analyzed by liquid chromatography tandem mass spectrometry (LC−MS/MS).

Liquid Chromatography Tandem Mass Spectrometry. Online liquid chromatography was performed by use of a Micro AS autosampler and Surveyor MS pump (Thermo Electron, Bremen, Germany). Peptides were loaded onto a 75-μm (internal diameter) Integrafrit (New Objective, USA) C8[42] resolving column (length 10 cm) and separated over a 40-min gradient from 0 to 40% acetonitrile (Baker, Holland). Peptides eluted directly (~350 nL/min) via a Triversa nanospray source (Advion Biosciences, NY) into a 7-T LTQ FT mass spectrometer (Thermo Electron), where they were subjected either to data-dependent CID or to targeted ECD.

Data-Dependent Collision-Induced Dissociation. The mass spectrometer alternated between a full FT-MS scan (m/z 395−1600) and subsequent CID MS/MS scans of the five most abundant ions. In the CID analysis of the phosphopeptide-enriched sample, if a neutral loss of 98 Da (49 or 32.67 m/z) from the precursor ion was observed in the five most abundant ions in the CID mass spectrum, an MS/MS/MS scan of the neutral loss ion was also acquired. Survey scans were acquired in the ICR cell with a resolution of 100 000 at m/z 400. Precursor ions were isolated and subjected to CID in the linear ion trap. The width of the precursor isolation window was 3 m/z. Only multiply charged precursor ions were selected for MS/MS. CID was performed with helium gas at a collision energy normalized to precursor m/z of 35%.[43] Activation q was 0.25. Precursor ions were activated for 30 ms. Dynamic exclusion was used with a repeat count of 2 and an exclusion duration of 120 s. Data acquisition was controlled by Xcalibur 2.0 software.

(42) Chi, A.; Valencia, J. C.; Hu, Z.-Z.; Watabe, H.; Yamaguchi, H.; Mangini, N. J.; Huang, H.; Canfield, V. A.; Cheng, K. C.; Yang, F.; Abe, R.; Yamagishi, S.; Shabanowitz, J.; Hearing, V. J.; Wu, C.; Appella, E.; Hunt, D. F. *J. Proteome Res.* **2006**, *5*, 3135–3144.

(43) Lopez, L. L.; Tiller, P. R.; Senko, M. W.; Schwartz, J. C. *Rapid Commun. Mass Spectrom.* **1999**, *13*, 663–668.
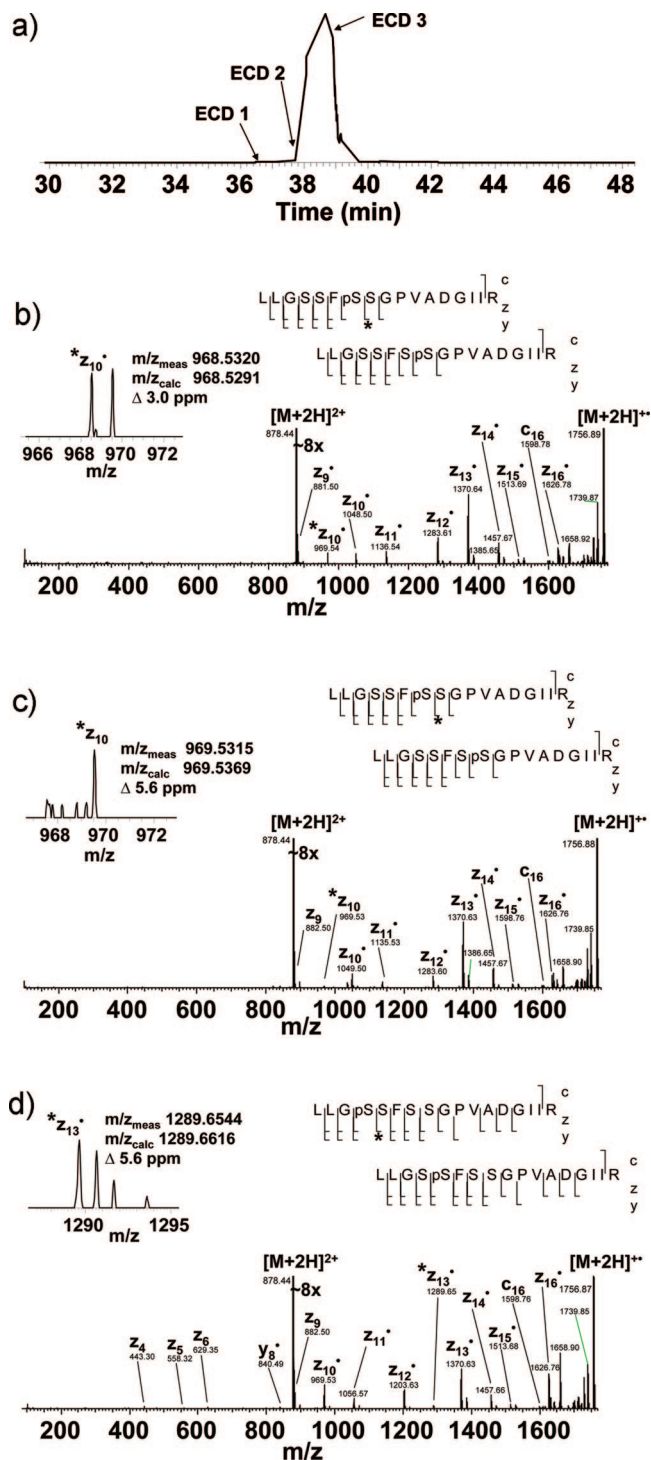
Figure 3. Online nanoLC targeted ECD of [M + 2H]²⁺ ions of phosphorylated LLGS¹³⁸SFSSGPVADGIIR. (a) Extracted ion chromatogram, showing elution of phosphorylated LLGS¹³⁸-SFSSGPVADGIIR, as [M + 2H]²⁺ ions. The arrows mark the selection of the precursor ions for ECD. ECD mass spectra of [M + 2H]²⁺ ions of phosphorylated LLGS¹³⁸SFSSGPVADGIIR at retention times (b) 36.5, (c) 37.7, and (d) 38.7 min. Insets show fragments observed and expanded views of *z_{10} and *z_{13}, indicating the presence of phosphorylated Ser141 and Ser138, respectively. ECD mass spectra comprise 24 coadded microscans.

DTA files were created from the CID data using Bioworks 3.3.1 (Thermo Fisher Scientific Inc.) (parameters: no scan grouping; minimum ion threshold of 15; absolute intensity threshold of 50). The DTA files were searched against the

Swissprot database (version 54.4; 287 050 entries) using the Mascot algorithm (Mascot version 2.2.03; http://www.matrix-science.com/; Matrix Sciences, UK). The search parameters used were as follows: human; fully tryptic (cleavage N-terminal to proline allowed); three missed cleavages allowed; carbamidomethylation as fixed modification; oxidation (M), deamidation (NQ), and phosphorylation (STY) as variable modifications; precursor accuracy of 50 ppm; fragment accuracy of 0.5 Da; instrument type ESI-Trap. The taxonomy filter resulted in 17 565 protein sequences being considered in the database search. Accepted identifications scored within the significance threshold ($p > 0.05$), except where noted (see Table 1), and had less than 10 ppm mass error. All CID identifications were confirmed by subsequent ECD data. Phosphorylation site localization from CID mass spectra was assessed using the A-score algorithm (http://ascore.med.harvard.edu/),[8] with manual validation.

Targeted Electron Capture Dissociation. The mass spectrometer acquired full FT-MS scans (m/z 395−1600) until the appearance of ions on an inclusion list triggered sequential CID and ECD MS/MS scans. Precursor ions were isolated in the ion trap and transferred to the ICR cell for ECD. Isolation width was 6 m/z. Automated gain control was used to accumulate sufficient precursor ions (target value 1e6, maximum fill time 1 s). The electrons for ECD were produced by an indirectly heated barium tungsten cylindrical dispenser cathode (5.1-mm diameter, 154 mm from the cell, 1 mm off-axis). The current across the electrode was ~1.1 A. Ions were irradiated for 60 ms at 5% energy (corresponding to a cathode potential of −2.775 V). Each ECD scan comprised either 8 or 24 coadded microscans, acquired with a resolution of 25 000 at m/z 400. Precursor ions for ECD fragmentation with 8 microscans were selected from an inclusion list containing the following m/z values: 423.22, 512.87, 530.74, 585.96, 639.33, 640.83, 666.32, 704.12, 817.39, 817.88, 828.87, 854.11, 878.44, 958.49. Precursors for fragmentation with 24 microscans were as above, with the omission of 423.22, 817.39, and 817.88, in order to focus on the Tyr55 phosphopeptide. The tolerance window for these parent ions was set at ±0.05 m/z. Dynamic exclusion was used with a repeat count of two and an exclusion duration of 30 s. ECD data were manually assigned, based on the known peptide sequences from the initial CID identifications.

RESULTS AND DISCUSSION

Human embryonic kidney cells were transfected with epitope-tagged human Sprouty2. After immunoprecipitation and SDS PAGE, the band corresponding to Sprouty2 was excised and subjected to in-gel trypsin digestion. The resulting peptide mixture was analyzed by standard LC−CID MS/MS, either directly or after phosphopeptide enrichment.[2] The phosphopeptides identified from these initial experiments are shown in Table 1. We have applied the recently developed Ascore tool to assist in phosphopeptide localization from CID mass spectra.[8] The Ascore algorithm is designed to automate the time-consuming process of manual site localization and to give a probabilistic score of the confidence in the localization. The Ascore is extremely useful, but we would urge caution in accepting all localized sites (scores >20) without manual analysis of the key differentiating fragment peaks, as ion trap spectra have a reasonable level of background noise, which may contribute to the localization score. Neutral loss dependent
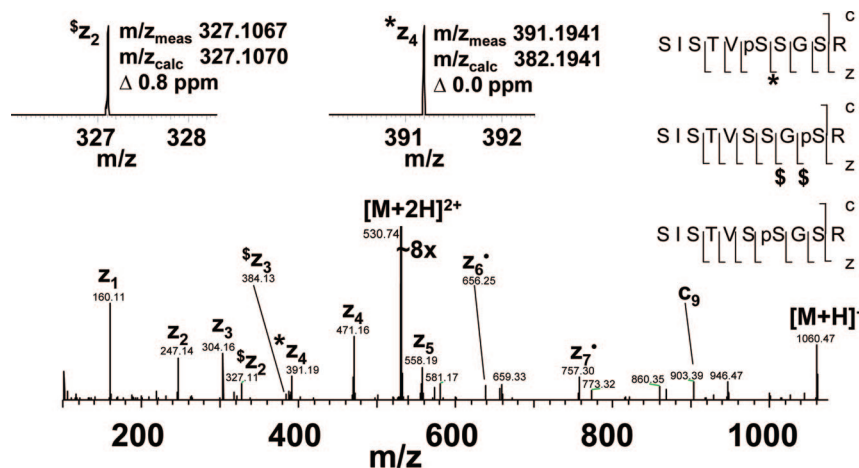
Figure 4. Online nanoLC targeted ECD of $[M + 2H]^{2+}$ ions of phosphorylated SISTVSSGS[118]R. Insets show observed fragments and expanded view of $^\$z_2$ and $^*z_4$, indicating the presence of phosphorylated Ser 115 and 118. ECD mass spectrum comprises 24 coadded microscans.

Table 2. Sprouty2 Phosphopeptides Identified from Initial LC–CID MS/MS and Targeted LC–ECD MS/MS

phosphopeptide	site	charge state	localized by ECD?	previously identified site?
R.AQpSGNGSQPLLQTPR.D	Ser 7	2	yes	no
R.AQSGNGSpQPLLQTPR.D	Ser 11	2	yes	no
R.AQSGNGSQPLLQpTPR.D	Thr 17	2	yes	no
R.DALTQQVHVLpSLDQIR.A	Ser 42	2	yes	no
R.NTNEpYTEGPTVVPR.P	Tyr 55	2	yes	yes[29]
R.NTNEYpTEGPTVVPR.P	Thr 56	2	yes	no
R.SISTVpSSGSR.S	Ser 115	2	yes	yes[33]
R.SISTVSpSGSR.S	Ser 116	2	yes	no
R.SISTVSSGpSR.S	Ser 118	2	yes	no
R.LLGpSSFSSGPVADGIIR.V	Ser138	2	yes	yes[33]
R.LLGSpSFSSGPVADGIIR.V	Ser 139	2	yes	no
R.LLGSSFpSSGPVADGIIR.V	Ser 141	2	yes	no
R.LLGSSFSpSGPVADGIIR.V	Ser 142	2	yes	no
K.SELKPGELKPLpSK.E	Ser 167	2	no	yes[33]
K.VPpTVPPR.N	Thr 305	2	yes	no

MS^3 spectra were also acquired in the CID experiment after phosphopeptide enrichment. MS^3 spectra for four of the seven phosphopeptides in Table 1 were obtained (data not shown); however, interpretation of these spectra was complicated by the potential for neutral loss of water from unmodified amino acids. MS^3 spectra were not used for phosphorylation site localization in this work.

Fifteen proteins were identified from the Sprouty2 gel band, in addition to Sprouty2, in the LC–CID MS/MS analysis without phosphopeptide enrichment (data not shown). Coelution of peptides similar in mass was observed in this experiment. Phosphopeptide enrichment reduced the sample complexity, allowing clean isolation of precursor ions. The enrichment step is particularly important for the ECD analysis (see below) as a larger isolation window (6 vs 3 m/z) is used to ensure sufficient ions are transferred to the ICR cell. In the ideal case of a completely purified small phosphoprotein, targeted site localization could be carried out without phosphopeptide enrichment. In practice, partial purification with additional phosphopeptide enrichment will often be the more straightforward option.

The phosphopeptides identified contain a total of 22 potential sites of phosphorylation. Putative site localization is shown in Table 1; however, for three out of seven peptides, the CID-based localization is ambiguous. The phosphopeptide containing Tyr55 is of particular interest, as phosphorylation of Tyr55 has been shown to be critical for Sprouty2 function.[29] It should be noted that the Tyr55-containing peptide in Table 1 is nontryptic, with cleavage occurring between arginine and proline.[44] A longer version of this peptide was identified in the analysis without enrichment, suggesting the acidic conditions of the phosphopeptide enrichment procedure may cause this fragmentation.[45] The CID mass spectrum of the Tyr55-containing peptide shows a dominant neutral loss of H_3PO_4, suggesting that the phosphorylation is on a threonine (Thr52 or Thr56) rather than Tyr55 (Figure 1). Unambiguous localization of the site of phosphorylation was not possible. Examination of the extracted ion chromatogram suggested that two versions of the peptide were present (Figure 1a); however, only the later eluting of these was selected for CID fragmentation.

In order to further examine the Tyr55-containing phosphopeptide and to confirm the localization of the other identified sites of phosphorylation, a targeted ECD analysis was carried out. The immunoprecipitation and phosphopeptide enrichment was repeated, and an inclusion list of the identified phosphopeptides (shown in Table 1) was used to restrict ECD events to the precursors of interest. Two targeted ECD analyses were carried out: one with 8 microscans per ECD spectrum and one with 24. The longer ECD events gave higher quality spectra for some low-abundance phosphopeptides, but results from both analyses were in agreement. In these analyses, both the earlier- and later-eluting Tyr55-containing phosphopeptide peaks were fragmented (Figure 2). The two mass spectra clearly show that the first-eluting peak corresponds to phosphotyrosine 55 (Figure 2a) and the second-eluting peak to phosphothreonine 56 (Figure 2b), a site of phosphorylation that has not been described previously. As with our previous NL ECD strategy,[26] the approach taken here is designed to maximize the advantages of ECD for phosphopeptide identification, specifically site localization, while minimizing the disadvantage of ECD (relatively long acquisition periods to achieve good-quality mass spectra from low-abundance precursors). In contrast to the NL ECD strategy, the targeted approach allows

(44) Keil, B. *Specificity of Proteolysis*; Springer-Verlag: Berlin, Germany, 1992.
(45) Olsen, J. V.; Ong, S. E.; Mann, M. *Mol. Cell. Proteomics* **2004**, *3*, 608–614.

Scheme 1. Human Sprouty2 Sequence, Showing Phosphorylation Sites Identified from Initial LC−CID MS/MS and Targeted LC ECD MS/MS[a]

1 MEARAQ**S**GNG	11 **S**QPLLQ**T**PRD	21 GGRQRGEPDP	31 RDALTQQVHV	41 L**S**LDQIRAIR	51 NTNE**YT**EGPT
61 VVPRPGLKPA	71 PRPSTQHKHE	81 RLHGLPEHRQ	91 PPRLQHSQVH	101 SSARAPLSRS	111 ISTV**SSGS**RS
121 STRTSTSSSS	131 SEQRLLG**SSF**	141 **SS**GPVADGII	151 RVQPKSELKP	161 GELKPL**S**KED	171 LGLHAYRCED
181 CGKCKCKECT	191 YPRPLPSDWI	201 CDKQCLCSAQ	211 NVIDYGTCVC	221 CVKGLFYHCS	231 NDDEDNCADN
241 PCSCSQSHCC	251 TRWSAMGVMS	261 LFLPCLWCYL	271 PAKGCLKLCQ	281 GCYDRVNRPG	291 CRCKNSNTVC
301 CKVP**T**VPPRN	311 FEKPT				

[a] Phosphorylation sites are in boldface type and underlined. Accession number O43597.

analysis of phosphopeptides that do not show a neutral loss, such as phosphotyrosine peptides. The targeted approach also allows lower abundance phosphopeptides to be selected for ECD, by omitting more abundant phosphopeptides from the inclusion list. In this experiment, there was a 200-fold difference between the intensities of the most abundant phosphopeptide and the least abundant (Supporting Information Figure 1). Targeted precursors can be specified with a mass tolerance small enough to make false positives unlikely, minimizing the possibility of spending time analyzing a nonphosphorylated peptide. ECD time can therefore be extended to maximize the information content obtained from the targeted phosphopeptides.

Figure 3 shows ECD mass spectra obtained from $[M + 2H]^{2+}$ ions of the LLGSSFSSGPVADGIIR phosphopeptide. The three mass spectra show that four separate isoforms of this phosphopeptide, with four distinct phosphorylation sites, are partially resolved by the LC separation. Figure 3b shows the ECD mass spectrum obtained at 36.5-min retention time. The fragments observed suggest that two isoforms of the phosphopeptide are present: one containing phosphorylation at Ser141 and one containing phosphorylation at Ser142. The defining fragment for the Ser141 phosphopeptide is $z_{10}^{\bullet}$ (denoted with * and enlarged in inset). Figure 3c shows the ECD mass spectrum obtained at retention time 37.7 min. The fragments observed suggest that the main species is the Ser142 phosphopeptide; however, a very low intensity z_{10} fragment (denoted with *) indicates the additional presence of the Ser141 phosphopeptide in low abundance. The complementary c ions are not observed, as is often the case for online LC-ECD of doubly charged tryptic peptides; however, the high mass accuracy and low noise level give added confidence to the Ser141 z_{10} assignment (see Figure 3b and c inset). Figure 3d shows the ECD mass spectrum obtained at retention time 38.7 min. The fragments observed suggest that two isoforms are present: the Ser138 phosphopeptide and the Ser139 phosphopeptide. The peak at m/z 1289.65 corresponds to the $z_{13}^{\bullet}$ fragment (denoted *) of the Ser138 phosphopeptide (see Figure 3d inset). The lower abundance of the $*z_{13}^{\bullet}$ fragment, relative to that of the $z_{13}^{\bullet}$ fragment from the Ser139 phosphopeptide, suggests that the Ser139 phosphopeptide is the main species present.

An important feature of the targeted strategy is that, in cases where different phosphorylation forms of a peptide approximately coelute (Figure 3), both the earlier- and later-eluting forms are sequenced because post-MS/MS dynamic exclusion is relaxed. This would not be the case if dynamic exclusion were applied after a single MS/MS event, as in many proteomic experiments. Where isobaric phosphopeptides coelute, composite spectra will be acquired. ECD mass spectra are typically acquired over a longer period than CID spectra. High-quality ECD mass spectra can be obtained in a few seconds; however, the time required is dependent on the precursor abundance. Lower abundance precursors require longer time to reach the target number of ions (accumulated in the linear ion trap), prior to the rapid ECD event. In this work, we have used up to 24 microscans, each with a maximum permitted fill time of 1 s, in order to obtain the highest possible quality ECD mass spectra from eluting phosphopeptides, i.e., performing ECD throughout the elution period of a peptide. These conditions favor the creation of composite spectra. However, interpretation of these spectra is not complicated, given that most of the fragments are identical and that loss of modifications from backbone fragments is not observed. Interpretation of the corresponding linear ion trap CID mass spectra would be more difficult, due to the potential for neutral losses of H_3PO_4, H_2O, and NH_3 from fragments and the lower resolution of the mass spectra. These difficulties were encountered during manual analysis of CID MS^3 spectra, where composite spectra of peptides phosphorylated at different sites were not distinguishable from neutral loss of H_2O from unmodified serine residues.

Figure 4 shows the ECD mass spectrum obtained from $[M + 2H]^{2+}$ ions of the phosphorylated SISTVSSGSR peptide. The fragments observed and their relative intensities suggest that this is a composite mass spectrum of three SISTVSSGSR phosphopeptides. The predominant species is SISTVSpSGSR (pSer116). The peaks observed at m/z 327.107 and 384.129 correspond to the z_2 and z_3 fragments of SISTVSSGpSR (pSer118; denoted with $). The peak observed at m/z 391.194 corresponds to the z_4 fragment of SISTVpSSGSR (pSer115; denoted with *). From this ECD mass spectrum, the sites of phosphorylation can be localized to serines 115, 116, and 118. The ease of analysis of composite ECD spectra is demonstrated in Figure 4, where fragment ion contributions from three phosphopeptides are evident.

The complete list of identified phosphopeptides is presented in Table 2. A total of 15 Sprouty2 phosphorylation sites have been identified. Targeted ECD has allowed the unambiguous assignment of 14 sites of phosphorylation (see Scheme 1), 11 of which are novel. A further phosphorylation site was identified by CID only. Mass spectra showing localization of the remaining sites are given in the Supporting Information.

ECD fragment ion abundances from large peptides have previously been used to quantify relative amounts of isomeric species;[46] however, this was from a direct infusion experiment.

(46) Pesavento, J. J.; Mizzen, C. A.; Kelleher, N. L. *Anal. Chem.* **2006**, *78*, 4271–4280.

While the mass spectrum shown in Figure 4 suggests that Ser116 is the major site of phosphorylation, it should be noted that coelution of the isomeric species may not be perfect (e.g., Figure 3) and that the yield of particular fragment ions in ECD may be influenced by structural effects.

CONCLUSIONS

We have shown that targeted ECD is a powerful technique for localizing sites of phosphorylation. Application of the strategy to human Sprouty2 increased the number of phosphorylation sites identified from 7 to 15, as well as providing increased confidence in site localization.

A similar targeted approach could be carried out using ETD in an ion trap instrument, as ETD has many of the same advantages as ECD. This would similarly benefit from retention of the labile phosphoamino acid intact, but give lower resolution spectra.

In summary, we have applied online liquid chromatography targeted ECD to the localization of 14 sites of Sprouty2 phosphorylation, 11 of which are novel. Prior to this work, only two novel sites of phosphorylation have been identified by ECD.[39,40] The unambiguous localization of the novel phosphorylation sites described here provides a basis for identification of the responsible kinases, and the functional significance of, Sprouty2 phosphorylation events. Further quantitative experiments to this end are ongoing in our laboratory.

SUPPORTING INFORMATION AVAILABLE

Additional material as noted in text. This material is available free of charge via the Internet at http://pubs.acs.org.